



A performance study of a high-torque induction motor designed for light electric vehicles applications

Pedro H. Camargos¹ · Ricardo E. Caetano¹

Received: 3 November 2020 / Accepted: 28 May 2021 / Published online: 21 June 2021
© The Author(s), under exclusive licence to Springer-Verlag GmbH Germany, part of Springer Nature 2021

Abstract

One of the biggest challenges for electric vehicle manufacturers is to properly choose the type of electric motor to be used. This choice impacts the performance of the other components in the electric propulsion system. This study analyzes the performance of the designed induction motor with application in a light vehicle electric propulsion system. Through simulations using Advanced Vehicle Simulator software, the torque performance of a designed induction motor was compared with the other two traction permanent magnet motors, also designed for light vehicle applications. The characteristics presented in the catalog for each machine were compared. Acceleration/deceleration test simulations were made for three different gradeabilities. The induction motor delivered higher torques than both permanent magnet machines for more than 80 % of the analyzed operation points. In the acceleration/deceleration tests, the designed induction motor presented higher instantaneous torques than those of the other permanent magnet machines. In the 4400 rpm to 6000 rpm overload region, the designed induction motor was more efficient than the permanent magnet machines. Therefore, this study shows that it is more advantageous to use this induction motor in light electric vehicle applications that require higher starting torques, such trajectories that contain ramps, and high slopes.

Keywords Drive cycle · Permanent magnet motor · Induction motor · Electric vehicle

1 Introduction

The first world conference on the environment was held in 1972 and was called the “United Nations Conference on the Human Environment”. There, countries from different continents created regulations to combat environmental pollution. In 1997 the Kyoto Protocol was signed, setting targets for reducing gas emission from burning fossil fuels. The transportation sector is responsible for consuming 61.4% of all oil consumed worldwide [17]. Replacing vehicles powered by internal combustion engines with electric vehicles would minimize the impacts of this sector on the environment.

The first electric vehicles were built in the nineteenth century. They used DC motor electric propulsion systems and

batteries with low autonomy. In the 1960s, 4.5 l of gasoline, corresponding to a mass of 4 kg, provided a range of 50 km. To store the same amount of useful electricity, it was necessary to use lead-acid batteries with masses up to 270 kg [13]. Since the 1960s, electric vehicles have become technically and economically viable due to the development of converters and electronic controllers and batteries with higher storage capacity. After the thyristor was invented in the 1950s, DC machines were gradually replaced by AC machines [8].

An overview of traction electric machines in drivetrains of electric vehicles, including small or light categories, [2], shows that two types of motors are predominant in electric propulsion systems: induction motor and permanent magnet [2]. The light vehicle electric propulsion system, a multivariable, nonlinear, robust coupling system, has several nonlinear system control methods, some of which have been proposed in Sun et al. [21–23].

Induction motor first came to the market in the first half of the twentieth century. By contrast, permanent magnet motors became technically viable in the 1950s with the development of new magnetic materials. Induction motors are robust,

✉ Pedro H. Camargos
pedro.camargos.eng@gmail.com

Ricardo E. Caetano
ricardoelias@unifei.edu.br

¹ Institute of Electrical and Energy Systems, Federal University of Itajubá, BPS Av. 1303, P.B. 50, Itajubá, MG 37500-903, Brazil

require little maintenance, [16,31,32], and have low manufacturing costs [11,12,19,24,26]. Permanent magnet motors are classified into two categories: brushless direct current motors (BLDC) and brushless alternating current motors (BLAC). The magnets can be positioned on, or inside, the rotor surface. Permanent magnet machines do not contain mechanical switching systems or rotor windings. They are light, small, and highly efficient machines, with high power density ratings with low acoustic noise [15,18,20].

From 1993 to 2013, almost 30% of the vehicles were built with induction motors, while 56% were built with permanent magnet motors [5]. Some traction motor manufacturers have been developing design techniques to improve the torque performance of the induction motor in electric traction applications. A new traction induction motors' stator winding configuration is proposed in Abdel-Khalik et al. [1]. These structures optimize machine torque production. A modified structure that maximizes the breakdown torque is also presented in Akhtar and Behera [4].

Studies carried out in Yang et al. [30] analyzed the different operating regions present in the efficiency map of an induction motor and the permanent magnet motor inside. The results showed that the induction motor has operational advantages, lower core loss, for example, than permanent magnet motors in some efficiency map zones. Another comparative analysis of these two types of motors was made in Ghazal and Jaber [10]. Using the same field-oriented techniques, the interior permanent magnet motor has a disadvantage against the induction motor presenting higher torque ripple compared to the induction machine drive.

The constructive characteristics of the electric motor are fundamental factors in choosing the type of traction motor. Motor racing competitions, such as Formula E, which use light, high-performance electric vehicles, require traction motors with high torque densities. Rallies and drag races are competitions with racetracks with steep slopes, requiring vehicles with traction motors that deliver high torques to the transmission system. In this scenario, the torque performance study of an induction motor (designed for light electric vehicle applications) provides research support for electric machine manufacturers and engineers.

The main objective of this article is to compare the torque performance of a designed induction motor to that of two permanent magnet machines. The three machines have the same application: propulsion system of light electric vehicles. This article is organized into seven sections. The induction motor, IM, was designed with specifications to operate in the propulsion system of electric vehicles. Section 2 presents the main characteristics of IM and the other permanent magnet motors. These traction motors are compared according to their catalog data in Sect. 3. Section 4 compares the performance of machines

through simulations. Finally, the conclusions are presented in Sect. 5.

2 Traction electric motors

2.1 Induction motor (IM)

Formula SAE electric is an automobile competition testing the performance of light electric vehicles. The IM is a traction motor developed for the electric propulsion system of Formula SAE light vehicles. It is an asynchronous cage machine with a nominal power rating of 6 kW. Its structure is shown in Fig. 1. The heat, generated by the losses inside the motor, is dissipated into the ambient air through the outer surface of the housing (air-cooled system). This machine is certified with an IP55 degree of protection and H class insulation. Therefore, it is protected from dirt, dust, water, and other corrosive materials. It can continuously operate at temperatures up to 180 °C (453.15 K) without resulting in damage.



Fig. 1 Induction motor (IM) structure. A machine used in the electric propulsion system of Formula SAE light electric vehicles

2.2 Brushless permanent magnet motor (PM-A)

The brushless permanent magnet motors (PM-A) were used in vehicles and light vehicles that participated in a Solar Powered Car Racing [27] competition. They have compact motors built with rare earth magnets, such as neodymium–iron–boron $\text{Nd}_2\text{Fe}_{14}\text{B}$ [9]. The machine has a double-speed switching system with two winding connection options (series or parallel). When operating in nominal conditions, the series connection allows the motor to deliver twice the nominal torque.

2.3 Interior permanent magnet (PM-B)

The permanent magnet motor (PM-B) is an electric motor that was developed for electrified drive axle of light electric vehicles (golf cars, electric bikes, and auto-rickshaw). The machine contains magnets located on the surface of the rotor. This structure protects against the effects of demagnetizing currents. It is a high-performance radial flow machine. It has an IP65 degree of protection, with protection against solid particles, with the same cooling system as the IM and PM-A.

3 Comparison using catalog data

The characteristics of IM, PM-A, and PM-B were compared according to the catalog data. The technical specifications can be found in Table 1. The region with operating points located between the nominal torque and the maximum torque curve is called the overload region. It is more advantageous to opt for IMs in applications that work in the overload region. In this region the IM has a maximum torque 1.7 times greater than the PM-A.

Motor efficiency maps were provided by the manufacturers (Fig. 2), and analysis was conducted on the perfor-

mance of the motor operating at specific speeds of rotation. Though efficiency–torque curves were obtained from efficiency maps, as shown in Fig. 3, it is possible to analyze the motor performance in the overload region. At 4000 rpm, within the overload region, the yield of the IM is greater than the PM-A operating points with torques greater than 18.34 (point *P*). At 4400 rpm the IM has greater machine efficiency than the both permanent magnet motors in applications with torques above 19 Nm. For the small torque range, in points between *Q*1 and *Q*2, the motor with the highest performance is the PM-B. With a fixed rotation at 6000 rpm, yields greater than 88% are obtained for torques greater than 12 Nm at point *R*1. At this speed the performance of IM is superior to that of PM-A and PM-B.

4 Comparison using electric vehicle simulator

The simulations were performed using the Advanced Vehicle Simulator (ADVISOR) software program. The software accurately models electric propulsion, auxiliary, and storage systems in electric vehicles. The objective was to compare the instantaneous and starting torques of the IM with those of the PM-A and PM-B when operating in a light and service electric vehicle and via acceleration/deceleration tests.

4.1 Advanced Vehicle Simulator

ADVISOR was developed in 1994 by the National Renewable Energy Laboratory (NREL). It is a tool used by researchers in many laboratories, institutes, and companies [7]. Companies like Ford, General Motors, and Daimler have already used ADVISOR in their project development processes. Electric vehicle propulsion, storage, and auxiliary system specifications and the driving cycle are the input data of the software.

The ADVISOR motor/controller model includes the inertia, volume, mass, and the efficiency map of the machine. In order for the vehicle to travel through the speed profile of the driving cycle, the torque T_{req} is required from the electric motor. The simulations use “backward-facing vehicle simulations” and “forward-facing simulations” that provide the instantaneous torque of the motor delivered to the transmission system. Values of T_m and the rotation speed Ω_m are outputs. The “backward-facing” simulations determine the torque and speed and power values required by the motor to comply with the speed profile of the driving cycle. The forward-facing simulations are responsible for T_m and the output power P_{out} . The sizing of the input parameters for the propulsion, auxiliary, and storage systems determines whether the motor will develop a torque T_m equal to T_{req} .

Table 1 Motor data

Parameter	IM	PM-A	PM-B
Continuous power [kW]	6	6	7
Continuous torque [Nm]	13	12	17
Nominal current [A]	120	140	167
Nominal voltage [V]	51	60	48
Nominal speed [rpm]	4400	6000	4000
Peak efficiency [%]	87	95	95
Peak power [kW]	20	11.2	9.5
Peak torque [Nm]	42.4	25	42
Weight [kg]	17	11.7	11
Moment of inertia [kg m^2]	0.0078	0.0070	0.0075

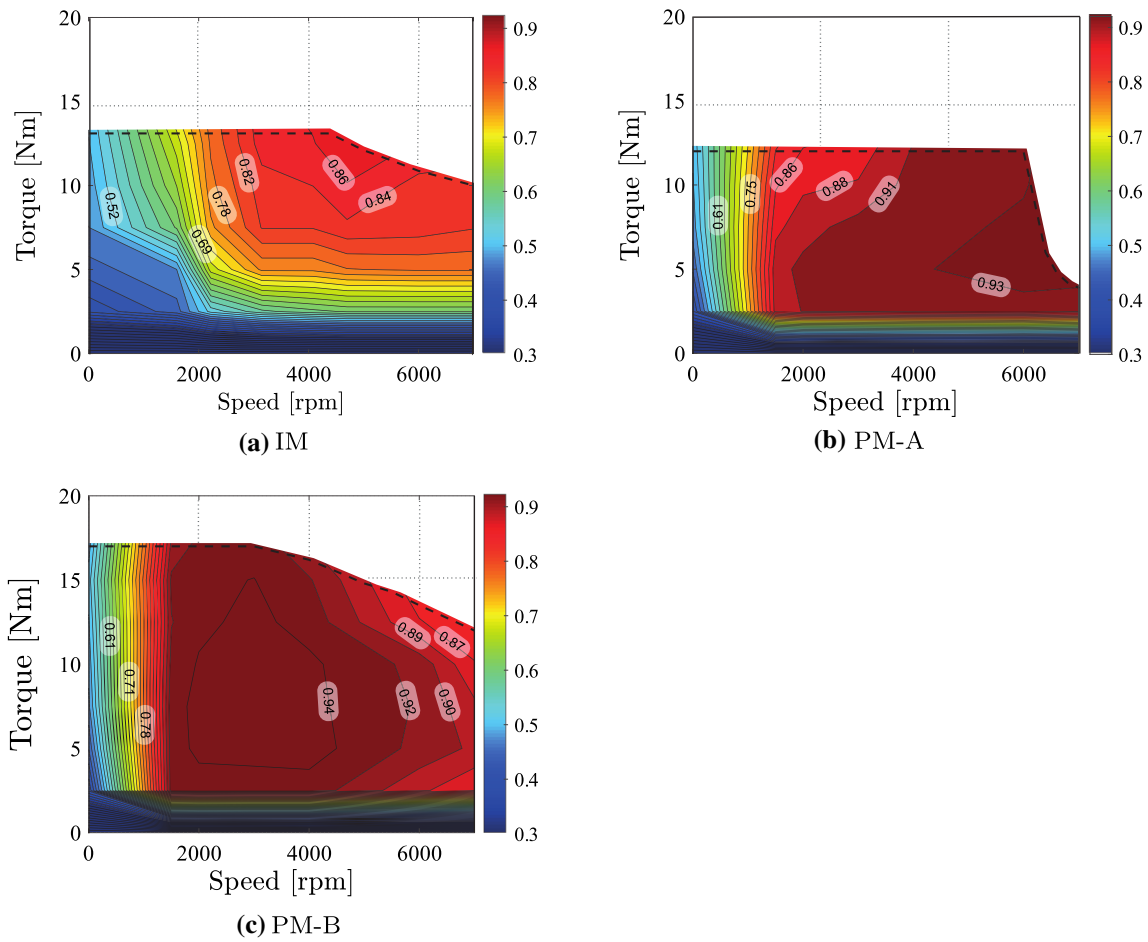


Fig. 2 Efficiency maps

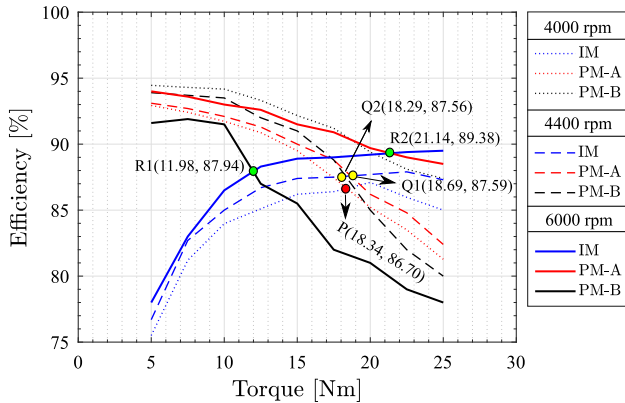


Fig. 3 Efficiency–torque curves

The T_m cannot exceed the maximum torque, T_{max} , supported by the machine.

Parameter T_m is calculated using Eq. (1), where P_{inp} is the input power, P_{aval} is the available power provided by the batteries, and J_m is moment of inertia. The T_{req} is limited to

the minimum value between the maximum motor torque and the minimum torque required to overcome the rotor inertia, T_i . Input power, P_{input} , is calculated using Eq. (3).

$$T_m = T_{req} \frac{P_{aval}}{P_{inp}} - J_m \frac{\Delta\omega_m}{\Delta t} \tag{1}$$

$$T_{req} = \min(T_i, T_{max}) \tag{2}$$

$$P_{inp} = P_{out} + P_{loss} \tag{3}$$

The output variables considered in the study were instantaneous torque, motor speed, operating points, and vehicle speed v . Vehicle acceleration, a , was calculated using Eq. (4). Variation in acceleration, Δa , is defined as the derivative of acceleration as a function of time, Eq. (5).

$$a(t) = \frac{dv}{dt} \tag{4}$$

$$\Delta a = \frac{da}{dt} \tag{5}$$

The torque difference ΔT_m responsible for varying acceleration over a time interval Δt equal to 1 s was calculated by:

$$\Delta T_m = T_{i+1} - T_i \tag{6}$$

where $i = 1, \dots, (t_{\max} - 1)$, t_{\max} is the maximum driving cycle time.

Table 2 Vehicle specification

Parameter	
Air density [kg/m ³]	1.20
Drag coefficient	0.60
Frontal area [m ²]	0.62
Vehicle mass [kg]	144.10
Wheel radius [m]	0.30
Drag coefficient	0.60

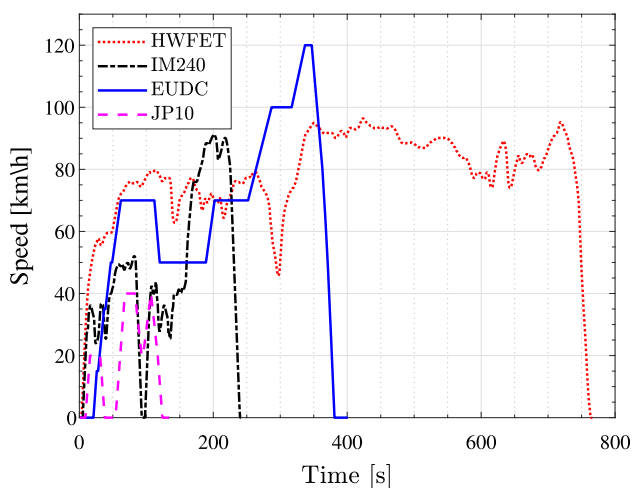


Fig. 4 Drive cycles

5 Working cycle simulation

Twelve simulations were carried out, four for each motor. All simulations used the same vehicle configuration. The vehicle specifications are shown in Table 2.

European and Japanese driving cycles are widely used in several countries in performance tests of electric and hybrid vehicles [25]. The driving cycles adopted in the simulations were: the EPA Highway Fuel Economy Test Cycle (HWFET), the Inspection and Maintenance Driving Cycle (IM240), the Extra Urban Driving Cycle (EUDC), and the Japanese 10 Mode (JP10). They are used in fuel emission testing for light-duty vehicles. The simulations used short and long driving cycles. JP10 had a maximum distance of 0.663 km, and HWFET had a maximum distance of 16.51 km. Figure 4 shows the curves for the driving cycles. The driving cycle for the vehicle in the EUDC simulation has a maximum acceleration of just 0.83 m/s². In the IM240 cycle, the car reaches acceleration 1.78 times higher than that of the EUDC cycle.

6 Acceleration/deceleration test

Vehicle acceleration/deceleration (A/D) tests are used in road design, vehicle traffic routes, pollutant emission assessments, and fuel consumption rate studies [6]. Therefore, it is possible to evaluate the performance of the A/D test by evaluating the instantaneous torque.

In the A/D test the vehicle traveled a route for 40 s. The acceleration/deceleration profile is shown in Fig. 5a. One of the constant acceleration models was described by Akcelik and Biggs [3], Yang et al. [28]. This model assumes that the speed increases at a constant rate throughout the acceleration and decreases at the same rate during the deceleration. The 0.41 m/s² acceleration value of the vehicle was used according to the Traffic Engineering Handbook and follows

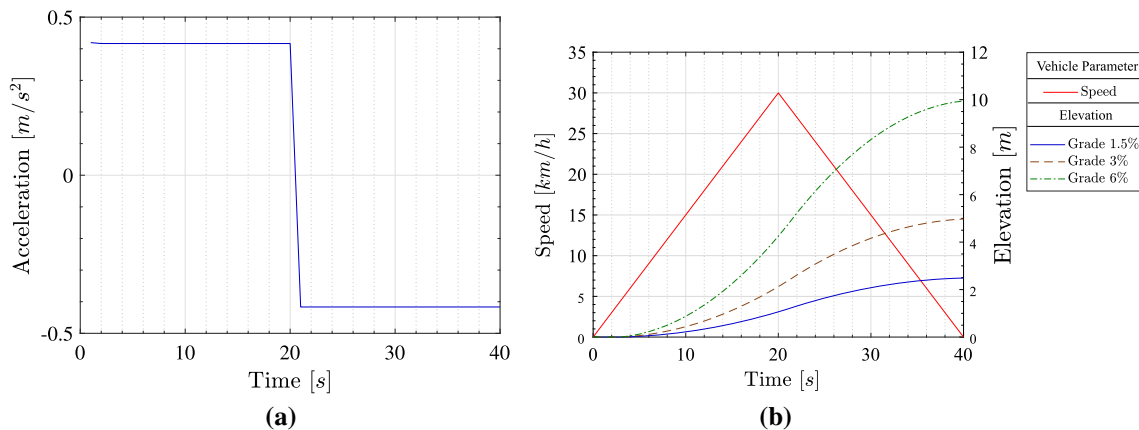


Fig. 5 Acceleration/deceleration test inputs **a** A/D profile, **b** speed–elevation

the guidelines stipulated by the Institute of Transportation Engineers (ITE) [29].

Equations (7) and (8) model the acceleration and deceleration profiles used in the A/D tests. The v_f, v_i are the vehicle’s final and initial speeds, respectively. The term t_a is the total time to reach v_f . The value of θ is the ratio between time, t , and instant of acceleration/deceleration starts, t_a .

$$a(t) = \frac{v_f - v_i}{t_a} \tag{7}$$

$$v(t) = v_i + (v_f - v_i)\theta \tag{8}$$

The degree of elevation of the road is quantified as the ratio between the vertical climb and the horizontal distance, and the ratio is positive for an uphill climb and negative for a downhill descent [14]. In the A/D tests, different slopes were used. Nine simulations were carried out, divided into three groups, A, B, and C. The A/D test was applied for slopes of 1.5%, 3%, and 6% for the simulations in groups A, B, and C, respectively (Fig. 5b). The instantaneous torque curves obtained in the tests were compared.

7 Results

7.1 Working cycle simulation

In each drive cycle, the electric vehicle was exposed to accelerations and decelerations, and the dynamic torque was required from the electric machine. The ordered pairs of torque and speed at each time of the drive cycle are called operation points. Vehicle operation points are shown in Fig. 6. The graphs in Fig. 7 show the percentage distribution of points in which the torque of the IM was greater than the torque, T_{PM} , of both permanent magnet motors.

The results of simulations for the HWFET driving cycle generated 766 points. In 83.3% of these, the torque of the IM, T_{IM} , was greater than the torque of both permanent magnet motors, T_{PM} , as shown in Fig. 6a. The torque of the IM was greater than that of the permanent magnet motors torque, PM-A and PM-B for more than 80% for drive cycle IM240. Simulations using EUDC and JP10 drive cycles, and torque performance of IM is also better. The IM did not deliver greater torques than the permanent magnet machines in only 14% of the 401 points in the European cycle. The

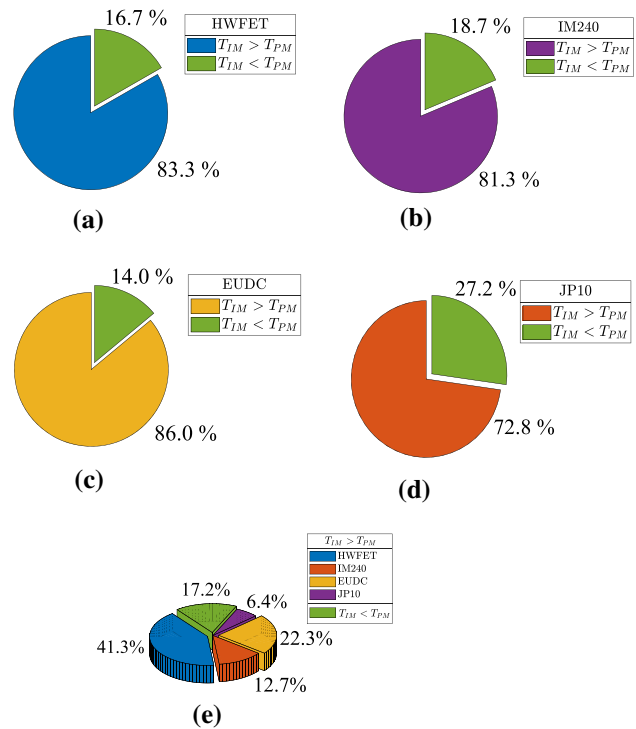


Fig. 7 Torque distribution electric motors. a HWFET, b IM240, c EUDC, d JP10, e all drive cycles

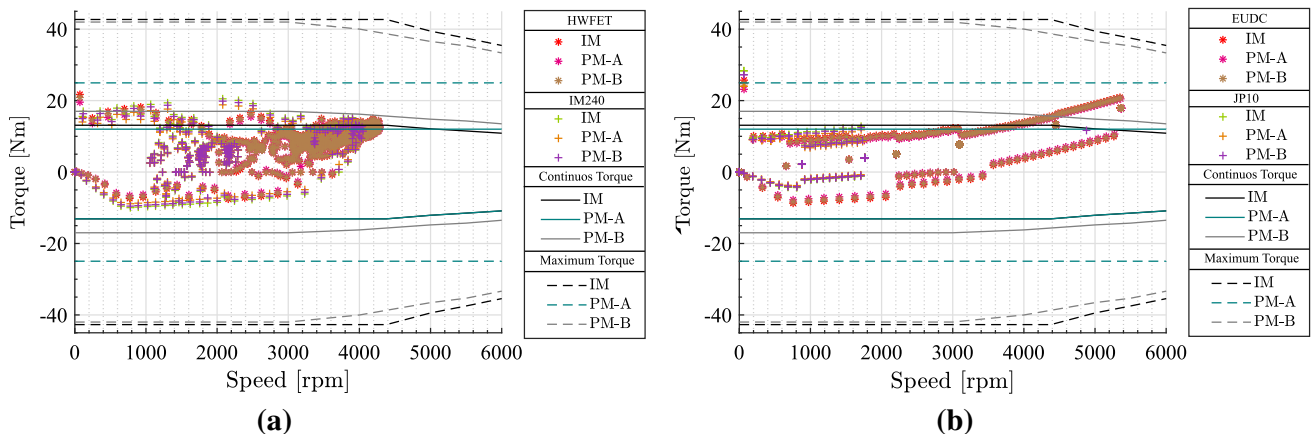


Fig. 6 Motors operation points per cycle a HWFET, IM240. b EUDC, JP10

IM delivered torques greater than the PM-A and PM-B in 72.2% of the points for the JP10 cycle. Considering all drive cycles, a total of 1545 points were obtained. Only in 17.2 %, the IM did not exceed both permanent magnet motors.

7.1.1 Instantaneous torque

The torque T_m for the IM was greater than that of the PM-A and PM-B in all driving cycles at the points of maximum acceleration/deceleration. The torque variations at the maximum and minimum points of Δa are shown in Fig. 8. Torque differences used to reach the specific vehicle acceleration variation, Δa , for each machine are ΔT_{IM} , ΔT_{PMA} , and ΔT_{PMB} , respectively. These torque differences IM performed better in all routes, with $|\Delta T_{IM}| > |\Delta T_{PMA}|$ and $|\Delta T_{IM}| > |\Delta T_{PMB}|$ at the points of maximum and minimum Δa .

7.1.2 Starting torque

The starting torque was obtained at the initial acceleration point. This occurred for $\Delta v \neq 0$ where the initial speed, $v_0 = 0$, was in the first seconds of the vehicle’s travel time. Table 3 shows the starting torques for all driving cycles. During the HWFET, IM240, and EUDC cycles, the IM had a starting torque approximately 11% higher than the PM-A and 4% higher than the PM-B. In the Japanese cycle, the starting torque of the IM was 18% higher than that of the PM-A and 4% higher than that of the PM-B.

7.2 Acceleration/deceleration test

Figure 9 shows the results of the A/D test. This figure is divided into three zones. The acceleration zone, $2 < t < 20$, comprises the increasing torque curves. In this case, the torque of the IM was higher than that of the permanent magnet machines for all simulation groups. The decreasing

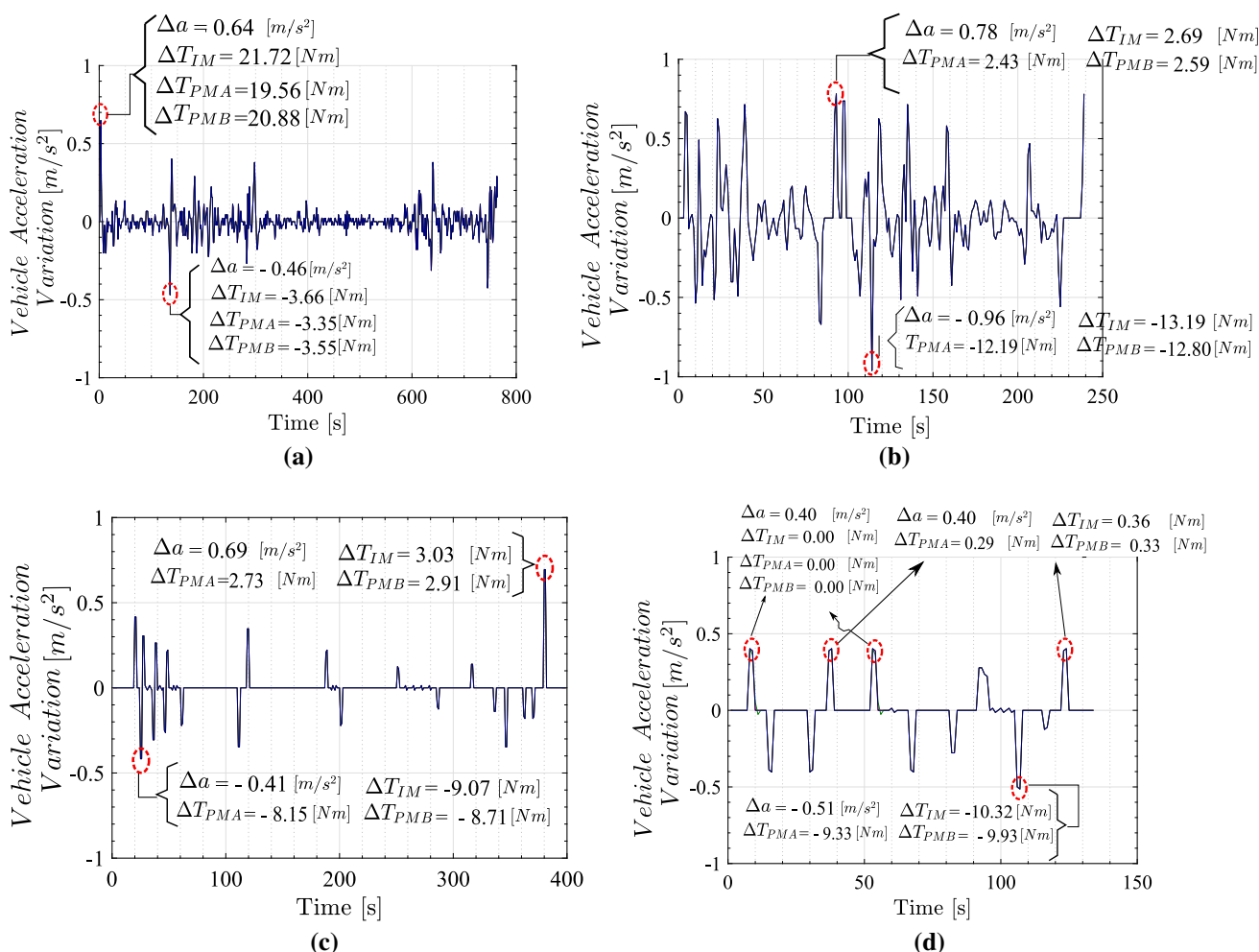
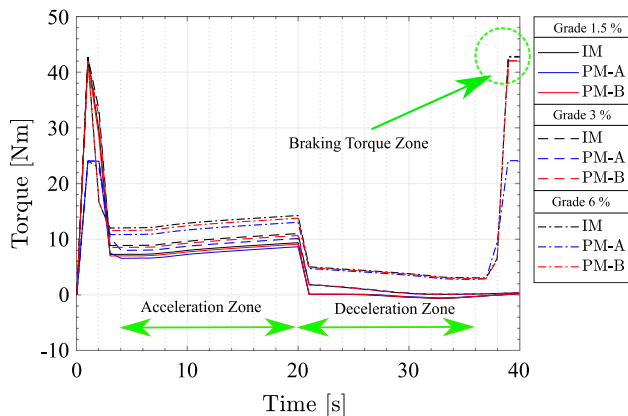


Fig. 8 Variation of vehicle acceleration with maximum and minimum acceleration and deceleration points per cycle. a HWFET. b IM240. c EUDC. d JP10

Table 3 Starting torque

Drive cycle	Δv [km/h]	Time [s]	T_{0IM} [Nm]	T_{0PMA} [Nm]	T_{0PMB} [Nm]
HWFET	1.60	4	21.72	19.56	20.88
IM240	2.41	6	15.57	14.01	14.96
EUDC	1.5	22	25.72	23.16	24.72
JP10	1.45	10	28.34	24.00	27.24

**Fig. 9** Torque A/D test

torque, $20 < t < 36$, is present in the deceleration zone. The decrease in torque occurred for all machines. The final moments of the vehicle tests evaluate the braking zone. For group C simulations, all motors were operated in the overload region. In this zone the torque of the IM was 56% higher than the PM-A and 1.68% higher than the PM-B.

One limitation is that the model was proposed for light electric vehicles only. This model can be used for other configurations for propulsion systems for light electric vehicles in future works.

8 Conclusion

Choosing the ideal motor for electric propulsion systems is a critical task. The simulation results showed that IM has a designer that provides better performance in overload regions than PM-A and PM-B. Even though there is another permanent magnet motor with better performance under overload, induction motors generally have a lower maintenance cost and are cheaper. The induction motor designed IM is ideal for use in applications that require high starting torques. A/D tests proved that the IM has a higher starting torque at higher slopes trajectories. In all the analyzed driving cycles, the IM was superior to the other two permanent magnet machines

presented, because IM operates with higher instantaneous torques in most of the analyzed operation points. Therefore, it is more advantageous to use IM than PM-A or PM-B in an electric propulsion system of small electric vehicles used in competitions like Formula SAE, rallies, and drag races. Working drive cycles A/D simulations provide comparative results that made it possible to obtain comparative results from the IM designed parameters. Manufacturers of traction electric machines and engineers can use the methodology used in this article to develop comparative studies to choose correctly the best traction motor for your drivetrain configurations.

Acknowledgements The authors are thankful to Improvement of Higher Education Personnel—Brazil (CAPES), for their support to this work.

References

- Abdel-Khalik AS, Massoud A, Ahmed S (2019) Nine-phase six-terminal pole-amplitude modulated induction motor for electric vehicle applications. *IET Electr Power Appl* 13(11):1696–1707. <https://doi.org/10.1049/iet-epa.2018.5796>
- Agamloh E, von Jouanne A, Yokochi A (2020) An overview of electric machine trends in modern electric vehicles. *Machines*. <https://doi.org/10.3390/MACHINES8020020>
- Akcelik R, Biggs DC (1987) Acceleration profile models for vehicles in road traffic. *Transp Sci* 21(1):36–54. <https://doi.org/10.1287/trsc.21.1.36>
- Akhtar MJ, Behera RK (2019) Optimal design of stator and rotor slot of induction motor for electric vehicle applications. *IET Electr Syst Transp* 9(1):35–43. <https://doi.org/10.1049/iet-est.2018.5050>
- Bazzi AM (2013) Electric machines and energy storage technologies in EVs and HEVs for over a century. In: *Proceedings of the 2013 IEEE international electric machines and drives conference, IEMDC 2013*, pp 212–219. <https://doi.org/10.1109/IEMDC.2013.6556255>
- Bokare PS, Maurya AK (2017) Acceleration–deceleration behaviour of various vehicle types. *Transp Res Procedia* 25:4733–4749. <https://doi.org/10.1016/j.trpro.2017.05.486>
- Cha KS, Kim DM, Jung YH, Lim MS (2020) Wound field synchronous motor with hybrid circuit for neighborhood electric vehicle traction improving fuel economy. *Appl Energy* 263(2019):114618. <https://doi.org/10.1016/j.apenergy.2020.114618>
- Chan CC (2002) The state of the art of electric and hybrid vehicles. *Proc IEEE* 90(2):247–275. <https://doi.org/10.1109/5.989873>
- Corporation S (1994) *Electric vehicle components USA (1994)*. http://www.evd1.org/docs/solectria_components_1994.pdf
- Ghazal A, Jaber Q (2019) Comparative analysis of induction motor and interior permanent magnet synchronous motor in electric vehicles with fuzzy logic speed control. *Jordan J Electr Eng* 5(4):202. <https://doi.org/10.5455/jjee.204-1582627568>
- Guneser MT, Dalcali A, Ozturk T, Ocak C, Cernat M (2016) An induction motor design for urban use electric vehicle. In: *Proceedings—2016 IEEE international power electronics and motion control conference, PEMC 2016*, pp 261–266. <https://doi.org/10.1109/EPEPEMC.2016.7752008>
- Kim B, Lee J, Jeong Y, Kang B, Kim K, Kim Y, Park Y (2012) Development of 50 kW traction induction motor for electric

- vehicle (EV). In: 2012 IEEE vehicle power and propulsion conference, VPPC 2012, pp 142–147. <https://doi.org/10.1109/VPPC.2012.6422627>
13. Larminie J, Lowry J (2003) *Electric vehicle technology explained*. Wiley, Hoboken
 14. Liu H, Rodgers MO, Guensler R (2019) The impact of road grade on vehicle accelerations behavior, PM2.5 emissions, and dispersion modeling. *Transp Res Part D: Transp Environ* 75(September):297–319. <https://doi.org/10.1016/j.trd.2019.09.006>
 15. Mi C (2006) Analytical design of permanent-magnet traction-drive motors. *IEEE Trans Magn* 42(7):1861–1866. <https://doi.org/10.1109/TMAG.2006.874511>
 16. Petrus V, Pop AC, Martis CS, Gyselinck J, Iancu V (2010) Design and comparison of different switched reluctance machine topologies for electric vehicle propulsion. In: 19th international conference on electrical machines, ICEM 2010, pp 1–6. <https://doi.org/10.1109/ICELMACH.2010.5608008>
 17. Pongthanasawan J, Sorapipatana C (2013) Greenhouse gas emissions from Thailand's transport sector: trends and mitigation options. *Appl Energy* 101:288–298. <https://doi.org/10.1016/j.apenergy.2011.09.026>
 18. Rosu M, Saitz J, Arkkio A (2005) Hysteresis model for finite-element analysis of permanent-magnet demagnetization in a large synchronous motor under a fault condition. *IEEE Trans Magn* 41(6):2118–2123. <https://doi.org/10.1109/TMAG.2005.848319>
 19. Sarlioglu B, Morris CT, Han D, Li S (2016) Benchmarking of electric and hybrid vehicle electric machines, power electronics, and batteries. In: Joint international conference—ACEMP 2015: Aegean conference on electrical machines and power electronics, OPTIM 2015: optimization of electrical and electronic equipment and ELECTROMOTION 2015: international symposium on advanced electromechanical motion systems (September), pp 519–526. <https://doi.org/10.1109/OPTIM.2015.7426993>
 20. Su GJ, McKeever JW, Samons KS (2001) Modular PM motor drives for automotive traction applications. In: IECON proceedings (industrial electronics conference), vol 3, no C, pp 119–124
 21. Sun X, Hu C, Lei G, Yang Z, Guo Y, Zhu J (2020a) Speed sensorless control of SPMSM drives for EVS with a binary search algorithm-based phase-locked loop. *IEEE Trans Veh Technol* 69(5):4968–4978
 22. Sun X, Wu J, Lei G, Cai Y, Chen X, Guo Y (2020b) Torque modeling of a segmented-rotor SRM using maximum-current-criterion-based LSSVR for torque calculation of EVS. *IEEE J Emerg Sel Top Power Electron*. <https://doi.org/10.1109/JESTPE.2020.297795>
 23. Sun X, Wu M, Lei G, Guo Y, Zhu J (2020c) An improved model predictive current control for PMSM drives based on current track circle. *IEEE Trans Ind Electron* 68(5):3782–3793
 24. Tabbache B, Kheloui A, Benbouzid ME (2010) Design and control of the induction motor propulsion of an electric vehicle. In: 2010 IEEE vehicle power and propulsion conference, VPPC 2010, no 1, pp 1–6. <https://doi.org/10.1109/VPPC.2010.5729102>
 25. Teoh JX, Stella M, Chew KW (2019) Performance analysis of electric vehicle in worldwide harmonized light vehicles test procedure via vehicle simulation models in ADVISOR. In: 2019 IEEE 9th international conference on system engineering and technology (ICSET). <https://doi.org/10.1109/ICSEngT.2019.8906356>
 26. Terras JM, Neves A, Sousa DM, Roque A (2010) Estimation of the induction motor parameters of an electric vehicle. In: 2010 IEEE vehicle power and propulsion conference, VPPC 2010. <https://doi.org/10.1109/VPPC.2010.5729252>
 27. Thacher EF (2015) *A solar car primer a guide to the design and construction of solar-powered racing vehicles*. Springer, New York. <https://doi.org/10.1007/978-3-319-17494-5>
 28. Yang G, Xu H, Tian Z, Wang Z (2016) Vehicle speed and acceleration profile study for metered on-ramps in California. *J Transp Eng*. [https://doi.org/10.1061/\(ASCE\)TE.1943-5436.0000817](https://doi.org/10.1061/(ASCE)TE.1943-5436.0000817)
 29. Yang G, Wang Z, Xu H, Tian Z (2018) Feasibility of using a constant acceleration rate for freeway entrance ramp acceleration lane length design. *J Transp Eng Part A: Syst*. <https://doi.org/10.1061/JTEPBS.0000122>
 30. Yang Z, Shang F, Brown IP, Krishnamurthy M (2015) Comparative study of interior permanent magnet, induction, and switched reluctance motor drives for EV and HEV applications. *IEEE Trans Transp Electrif* 1(3):245–254. <https://doi.org/10.1109/TTE.2015.2470092>
 31. Zeraoulia M, Benbouzid MEH, Diallo D (2006) Electric motor drive selection issues for HEV propulsion systems: a comparative study. *IEEE Trans Veh Technol* 55(6):1756–1764. <https://doi.org/10.1109/TVT.2006.878719>
 32. Zhu ZQ, Chan CC (2008) Electrical machine topologies and technologies for electric, hybrid, and fuel cell vehicles. In: 2008 IEEE vehicle power and propulsion conference, VPPC 2008, pp 1–6. <https://doi.org/10.1109/VPPC.2008.4677738>

Publisher's Note Springer Nature remains neutral with regard to jurisdictional claims in published maps and institutional affiliations.